Earth and Planetary Science
https://ojs.nassg.org/index.php/eps

REVIEW

Main Mechanisms of Celestial Bodies Negative Polarization Formation: A Review

Dmitry Petrov

Crimean Astrophysical Observatory (CrAO RAS), Nauchnyj, 298409, Crimea

ARTICLE INFO

Article history
Received: 27 March 2023
Revised: 24 April 2023
Accepted: 28 April 2023
Published Online: 17 May 2023

Keywords:
Light scattering
Degree of linear polarization
Polarization mechanisms

ABSTRACT

The scattered light by the vast majority of celestial bodies without atmospheres has a characteristic feature: A negative branch of linear polarization degree at little phase angles. Researchers have proposed many theoretical mechanisms to explain this feature. This review describes the main mechanisms that form a negative branch of linear polarization degree. The results of ground-based observations of the negative branch of the degree of linear polarization of various objects of the solar system are described. Scattering by single particles, shadow effect, coherent backscattering enhancement, and effects of the near field are considered. The review will be useful for all researchers studying the scattering of light by celestial bodies.

1. Introduction

Consider light with wavelengths lying in the optical range. Light incident on a scattering object is generally unpolarized. However, the scattered light is partially polarized, that is, there are planes in which the predominant part of the oscillations of the electrical vector of the electromagnetic wave is concentrated. Typically, the scattered light intensity is decomposed into two components. The first of them, denoted by $I_\parallel$, means the scattered radiation intensity polarized in the plane of scattering (the plane containing the observer, the scattering object and the light source). The second, denoted by $I_\perp$, means the intensity of scattered light whose polarization is in a plane, which is perpendicular to the plane of scattering. The linear polarization degree, expressing the relationship between these two quantities, is determined by the formula:

$$P = \frac{-I_\parallel + I_\perp}{I_\parallel + I_\perp}, \tag{1}$$

If $I_\perp > I_\parallel$, the linear polarization degree is positive. Otherwise, it is negative. The linear polarization degree depends on the phase angle α (the angle between the direction of the scattering object and the light source, and the scattering object—the observer).

The dependence of linear polarization degree on phase

*Corresponding Author:
Dmitry Petrov,
Crimean Astrophysical Observatory (CrAO RAS), Nauchnyj, 298409, Crimea;
Email: dvp@craocrimea.ru

DOI: http://dx.doi.org/10.36956/eps.v2i1.831

angle has been widely studied. At phase angles of 0-30°, laboratory measurements of vast majority of surfaces consisting of small particles, as well as polarimetric observations of most objects of the solar system visible from our planet, show a region of negative polarization, which often coincides with the brightness opposition effect. Characteristically, the size of the negative polarization region, as well as its magnitude, depends on the physical properties of the scattering objects [1].

Phase dependence of linear polarization degree negative branch can be described by the values shown in Figure 1: P_{min} is the minimal value of the degree of polarization; α_{min} is the phase angle at which the minimum polarization is observed; α_{inv} is the angle of inversion at which the polarization equals to zero; $h = \left.\frac{dP}{d\alpha}\right|_{\alpha=\alpha_{inv}}$ is the polarization slope; P_{max} is maximum polarization degree; α_{max} is the angle of maximum polarization. All these quantities depend very strongly on the parameters of the scattering object and, therefore, are applicable in the interpretation of observational data.

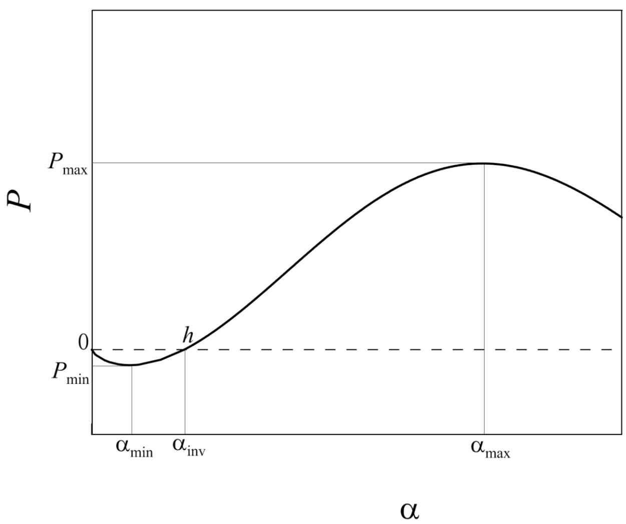

Figure 1. Characteristic form and main parameters of the phase dependence of the degree of linear polarization.

For non-atmospheric bodies, negative polarization branch curves usually look like a parabola ($\alpha_{inv} \approx 2\alpha_{min}$), which, for example, are observed on the Moon [2,3]. The negative polarization is also regularly observed in the moons of Jupiter and Saturn, although their curves show a marked dissymmetry in the negative polarization branch. Measurements of the linear polarization degree of various samples in the laboratory show huge variety of negative polarization [4].

The variety of phase curves is explained by a sufficiently large number of physical mechanisms that cause negative polarization. Lyot, who discovered the negative polarization of the Moon, described three main groups of physical principles underlying these physical mechanisms [2]:

- many reflections between scattering objects;
- output light refractions on transparent or translucent objects;
- light diffraction.

The first specific model describing the mechanism of the occurrence of negative polarization and corresponding to the first Lyot hypothesis is probably owing to Ohman [5]. The Ohman model uses double reflection from the troughs on a rough scattering surface, which can create negative polarization and oppositional effects. However, the experimental nature of the model was emphasized by the author, despite its progressiveness at that time.

Studies within the framework of the second Lyot group were launched by McCoyd [6]. McCoyd's research focused on a two-dimensional model that studied the behavior of light with a single external reflection and two refractions, accompanied by total internal reflection, from a uniform surface layer bounded by two interfaces.

Hopfield [7] was the first to attempt a model based on Lyot's third hypothesis using Sommerfeld's theory of diffraction. Although the model was only approximated, it gained popularity (see for example Veverka [8] and references within). The applicability of Hopfield's approach to non-atmospheric surfaces is currently unknown.

Specific mechanisms (some of which are still debatable) for the occurrence of negative polarization can be roughly divided into the following groups: Scattering by single particles, shadow effect, coherent backscattering enhancement, and the near field effects. Below we will try to describe at least some of the models underlying each of these mechanisms.

There are a number of works in which a review of certain mechanisms underlying the scattering of light has been carried out. Of particular note is the review [9], which describes achievements in the theory of light scattering by morphologically complex objects, as well as their application to the interpretation of observational data obtained in the course of photometric and polarimetric observations of celestial bodies. However, only in this review, the main mechanisms are brought together.

Note that we will focus on describing such mechanisms that can be described theoretically. Recently, a huge number of computer simulation methods have appeared that make it possible to calculate the characteristics of scattered light numerically. For example, numerical codes for modern Monte Carlo radiative transfer codes can be applied to each described negative polarization mechanism. However, there are so many variations of numerical methods that their detailed description is far beyond the scope of this review. A recent review provides a complete description of modern Monte Carlo radiative transfer codes [10] and references within.

2. Negative Polarization in Ground-based Observations of Celestial Bodies

Ground and space observations of the bodies of the Solar System (the Moon, regolith surfaces of planets, comets, asteroids, satellites of giant planets, etc.) can provide a huge variety of information about the polarization of light scattered by them in a wide range of phase angles and wavelengths [11]. The phase dependences of brightness and polarization obtained from photopolarimetric observations of celestial bodies have a number of features that can be used to obtain information on the scattering properties of individual particles, their composition, structure, and also on the parameters of the medium. Almost all observed celestial bodies have a negative polarization branch, but the depth, position, and shape of this branch differ markedly for different objects.

Lyot [12] was the first to discover that the disk-integrated polarization of the Moon, as well as its local regions, becomes negative at phase angles of about 23°. In addition, polarimetric observations of the Moon were carried out by many researchers [13,14]. In these works, it was shown that the main properties of the negative branch of polarization for the Moon are as follows:

1) The negative polarization branch for the entire Moon is almost symmetrical with the parameters $P_{min} = -1.2\%$, $\alpha_{min} = 11°$, $\alpha_{inv} = 23.6°$;

2) Lunar objects of different morphology have different P_{min} values in the range from –0.6% to –1.4%. Low values of negative polarization are characteristic of light continents, while dark seas have large P_{min};

3) The dependence of P_{min} on the surface albedo for various lunar formations has a horseshoe shape: At low albedos, P_{min} increases with albedo, but then begins to decrease;

4) The absolute value of P_{min} for bright craters does not depend on the wavelength, but slightly increases with increasing wavelength for dark material;

5) The inversion angle slightly increases with increasing wavelength.

Multiple polarimetric observations of the Galilean satellites of Jupiter in UBVR filters at phase angles in the range from 11.8° to almost 0° made it possible to obtain almost all polarimetric information available in the course of ground-based observations of these objects [15-19].

In these works, both phase and longitudinal and spectral dependences of the degree of linear polarization were studied. Some systematic differences have been found in the depth of the negative polarization branch for Io, Europa, Ganymede, and Callisto. Large longitudinal variations in the degree of polarization were found for Callisto and Io, while they were noticeably smaller in the case of Ganymede and Europa. The polarization minima for the trailing hemispheres of Io, Europa, and Ganymede turned out to be systematically higher than for the corresponding leading hemispheres. However, the leading hemisphere of Callisto has noticeably higher polarization values and large α_{min} in all spectral ranges compared to those of the trailing hemisphere. Separation of phase and longitudinal polarization effects was performed for Ganymede [16] and Callisto [20].

In addition, an opposite effect of polarization was found in the form of a sharp increase in negative polarization at extremely small phase angles $\alpha \approx 0.5$-$0.7°$ in combination with the usual behavior of the negative branch of the degree of linear polarization for Io, Ganymede and Europa [17,18,21]. This phase angle is comparable to the width of the brightness peak observed for Europa, indicating that both opposition phenomena are likely caused by the backscattering coherent backscattering mechanism [17].

A small number of observations were devoted to measurements of the degree of polarization of three satellites of Saturn: Dione, Iapetus and Rhea [22,23]. The results turned out to be sufficient for estimating the depth of the negative polarization branch, but it was not possible to determine the inversion angle. Rhea and Diona have close P_{min} values close to –0.4%. For Iapetus, the negative branch turned out to be much deeper for the dark leading hemisphere ($P_{min} = -1.3\%$) than for the light trailing hemisphere ($P_{min} = -0.2\%$).

The phase dependence of the degree of linear polarization of comets was measured (for different comets) in the range 0.3-122°. The phase dependence turned out to be smooth, similar to the phase curves of non-atmospheric bodies of the Solar System. All comets exhibit a shallow branch of negative polarization in the backscattering region, first discovered by Kiselev and Chernova [24], which inverts into positive polarization at $\alpha \approx 21°$ with a polarization slope at the inversion point $h \approx 0.2$-$0.4\%/°$, after which the positive branch of polarization with a broad maximum at angles α_{max} of about 90°-100° appears as comets. While the minimum value of the degree of linear polarization is usually –2% [25-27], a significant scatter of data for different comets is observed at $\alpha > 40°$. Dlugach et al. [28] and Halder & Ganesh [29] showed that computer simulation of light scattering processes by particles of a heterogeneous structure is able to reproduce the phase curves of the degree of linear polarization of most comets.

Lyot [30] was the first to measure the degree of polarization of light scattered by asteroids. He found that the asteroids 1 Ceres and 4 Vesta show the same negative polarization at low phase angles as the Moon, Mars and Mercury. An extensive program of polarimetric observations has been carried out by Zelner et al. [31], Zellner and Gradie [32] and many other researchers, resulting in the collection of a large amount of polarimetric observational data that can be found in the polarimetric asteroid database①. For asteroids, the negative polarization branches are very diverse. The angle of inversion for different asteroids varies from 16 to 25 degrees. The value of the minimum $|P_{min}|$ for C-type asteroids reaches 2.1%, for E-type asteroids this value is about 0.5%. In the work [33] it was shown that the negative polarization branch of some asteroids, such as asteroid 419 Aurelia, can be reproduced by computer simulation of light scattering by analog of planetary regoliths.

Summing up this section, we can say that the observational data on the degree of linear polarization of objects in the solar system demonstrate a huge variety of phase polarization curves, which indicates a great variety of physical mechanisms for the formation of the negative branch of the degree of linear polarization.

3. Models of Negative Polarization Formation

Single particles can produce the negative polarization branch of scattered light. This feature has been repeatedly established both in the course of calculations performed according to the Mie theory [34], in the course of polarimetric observations of cometary atmospheres [35], in measurements of the linear polarization degree of singly scattered light in the laboratory [36,37], and also in the course of computer simulation of light scattered from single particles of irregular shape [38]. It should be noted that a single particle is understood as an object of an arbitrarily complex structure, sufficiently remote from other similar objects. Inside a single particle, acts of multiple scattering of light between its elements can occur, but there is no multiple scattering between different particles, or their contribution is negligible. Let us describe main mechanisms capable of inducing negative polarization in single particles.

3.1 Ohman Model

The Ohman model considers double reflections from two mutually perpendicular planes forming a trough, the cross section of which is a right triangle [5]. The emerging negative polarization looks like this: a triangular trough has the well-known property of reflecting light in the strictly opposite direction. When the axis is perpendicular to the scattering plane, it exhibits a trough property, but this property disappears when the axis is parallel to the scattering plane. The chute axis may have an intermediate orientation, resulting in non-zero phase angles. In the case when the axis of the trough is perpendicular to the plane of scattering, the doubly reflected rays have a positive polarization and cannot be observed at nonzero phase angles. On the other hand, when the axis of the trough is parallel to the plane of scattering, the negative polarization of doubly reflected beams predominates, but these beams are also observed at nonzero phase angles. As a general rule, negative polarization should be maintained for all but zero phase angles when averaged over all trough orientations. But, on the other hand, the light reflected once from the trough is positively polarized. Because the negative polarization of light is more noticeable at small phase angles, and the positive polarization of light is more noticeable at large phase angles, the polarization curve shown in Figure 1 can be obtained.

3.2 Steigmann Model

The Steigmann model [39,40] uses single and double reflection, approximating the scattering media by cylindrical pits with a flat bottom, where diameter and density are inversely related. The axes of the pits can be tilted from 0° to 90° towards the incident rays. The light undergoes two Fresnel reflections inside the pits, either from the floor and wall, or vice versa. The floor and walls of these pits act as reflectors, as in the Ohman model described earlier. Consequently, such reflections in the pits favor the appearance of negative polarization.

The Steigman model uses parameters such as the surface substance refractive index, the pit radii range, the reflection coefficient, and the depolarization coefficient to model the surface albedo and has shown good agreement with the experimental data of celestial bodies and laboratory studies [41,42]. Unlike the Wolf model (see Section 3.4), Steigman's model does not predict the second branch of negative polarization resulting from shading at significant phase angles. The Steigman model contains non-parabolic theoretical polarization curves, which indicates the variability of the experimental curves, described above.

3.3 The Contribution of Multipoles

If the scattering particle is much smaller than wavelength, then it can be considered an electrostatic dipole that scatters light in accordance with Rayleigh's law. The linear polarization degree of scattered light by a Rayleigh particle

① Lupishko, D., Ed. (2022). Asteroid Polarimetric Database V2.0. urn:nasa:pds:asteroid_polarimetric_database::2.0. NASA Planetary Data System. Available from: https://sbn.psi.edu/pds/resource/apd.html is described by the following well-known formula:

$$P = \frac{1-[\cos\alpha]^2}{1+[\cos\alpha]^2}, \tag{2}$$

where α is phase angle.

This polarization is always positive. However, when the light-scattering object is of considerable size, the participation of multipoles should be taken into account. It is commonly believed that for spherical particles it is multipoles that lead to negative polarization. For particles of arbitrary shape, estimating the multipoles contribution is a rather difficult task. Nevertheless, important results can be achieved for small degrees of multipolarity. It was demonstrated by Shkuratov et al. [43] that the following formula is valid, which describes sum radiation of magnetic dipoles, quadrupoles and ordinary dipoles:

$$P = \frac{[1+(M-D)\cos\alpha]^2 - [M+\cos\alpha - D\cos 2\alpha]^2}{[1+(M-D)\cos\alpha]^2 + [M+\cos\alpha - D\cos 2\alpha]^2}, \tag{3}$$

where M and D are the contribution of the magnetic dipole and quadrupole moments to the total emission compared to the dipole emission. At M = D = 0, Equation (3) turns into Equation (2). Equation (3) can predict the negative polarization branch for certain combinations of D and M, which depend on the size, optical constants, and structure of the light-scattering particles. Figure 2 shows the α_{inv} dependence on the parameters D and M. It can be seen from the figure that combinations of these parameters are quite capable of well describing the actually observed inversion angles from 15 to 30 degrees.

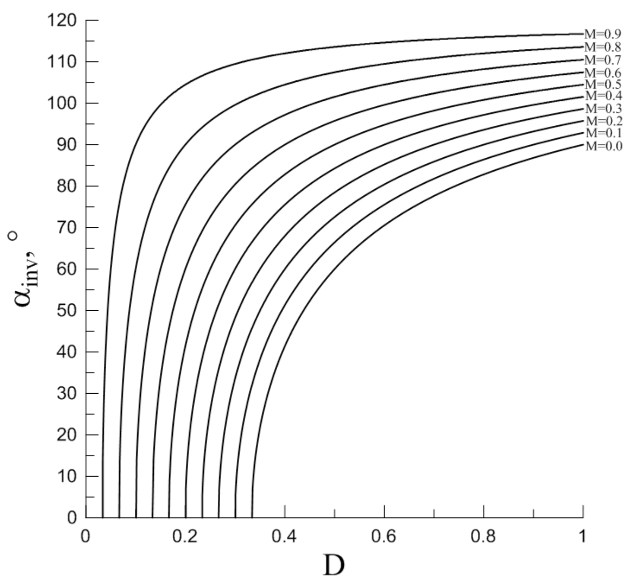

Figure 2. The inversion angle (α_{inv}) dependence on the parameters D and M of Equation (3).

3.4 Wolff Shading Model

Wolff [44] took up the studying of Lyot's first conjecture. He suggested a model that takes into account single and double light scattering [45,46], which, apparently, is in agreement with observations. Wolff studied a scattering medium consisting of particles, but at the same time having a rough surface. He suggested that the shading of a certain proportion of particles due to the roughness of the interface contributes to negative polarization (Figure 3). In particular, Wolff suggested that for positively and negatively polarized pairs of rays (1', 2') and (3', 4'), respectively, the differences in the probability of propagation of rays (ray 2' will leave the medium with a lower probability than the rest of the rays) lead to negative polarization. Due to the peculiarities of light scattering by Rayleigh particles, light scattered along conjugate paths involving particles 3 and 4 is negatively polarized, and scattered along paths involving particles 1 and 2 gives a positive polarization. Because of waves lying in the scattering plane (1-2) are less likely to leave the surface (in particular, wave 2' in Figure 3) than waves in a plane perpendicular to the scattering plane (3-4), negative polarization will dominate.

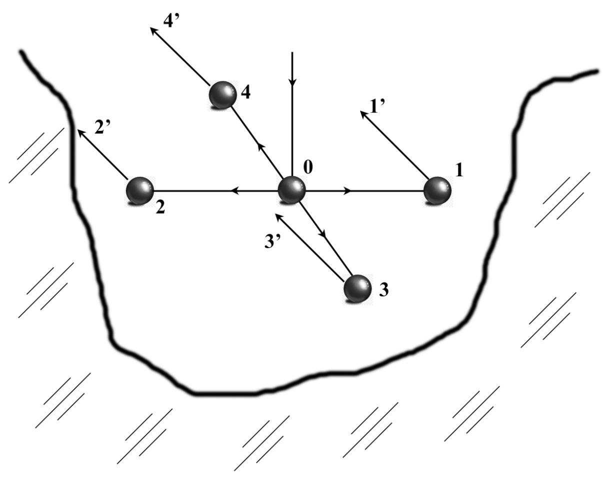

Figure 3. Wolff shading model. Wave 2' will leave the medium with a lower probability than the rest of the waves.

The following parameters are used in the Wolf model: The complex refractive index of scattering objects m = n + ik, the ratio of the width to the depth of emptinesses between particles, the average particle size used to calculate the scattering of unpolarized light and the intensity ratio of singly and doubly scattered light, which is influenced by the structural properties of the scattering medium. Wolff's model has been validated through laboratory tests [47] and applied to explain data from the planets [48,49].

Shkuratov [50] simplified the Wolff shading model under the assumption of a small-angle approximation. For the linear polarization degree, the following equation was obtained:

$$P = C_1\left[\frac{(n-1)^2}{An^2(n+1)^2} + C_2\frac{(n^2-1)^2}{(n^2+1)^2}\right]\alpha^2 - C_3\frac{(n^2-1)^2}{(n^2+1)^2}\alpha, \quad (4)$$

where A is the geometric albedo of the surface, n is a real part of refractive index, C_1, C_2 and C_3 are parameters describing the asymmetry of beams 1-4 due to shading (Figure 3). Equation (4) is applicable only for sufficiently small phase angles $\alpha < 30°$.

3.5 McCoyd Model

Consider a medium formed by a complex, large-scale structure. In scattered light, two components can be distinguished—on the surface layer there is one reflection, and in the depth of the layer there are multiple refractions and reflections. McCoyd [6] investigated the polarization of light reflected and refracted both outside and inside a layer having a rough surface and a smooth lower boundary separating this layer from another layer, less optically dense. Using the assumption of Fresnel reflection coefficients, the Monte Carlo method was used for calculations.

McCoyd suggested that the negative polarization might be the result of total internal reflection at the bottom interface between the layers and refraction at the top interface. However, this model is not suitable for interpreting observations of extra-atmospheric celestial bodies and laboratory measurements, as was shown by Shkuratov et al. [51].

3.6 Hopfield Model

Hopfield [7] assumed that shadowing in a scattering medium composed of dust particles could explain the negative polarization through the Sommerfeld diffraction mechanism. The edges of dust grains are considered to be fine half-planes of an ideal conductor, and in the shadow zone below them, a diffracted electromagnetic field with negative polarization is reflected to the observer by scattering surface elements lying under them.

Hopfield's calculations suggest that the Moon's minimum polarization (–1.2%) may be due to tiny 5 μm particles located close together, although it is not clear if the equations used are appropriate for lunar particles. On the one hand, an electromagnetic field diffracted by a half-plane at a distance of several wavelengths has not only a transverse, but also a longitudinal component of the electromagnetic field. For this reason, it is not entirely clear whether it can be described by the usual linear polarization degree.

On the contrary, it was shown that the diffracted field in the wave zone at diffraction angles greater than 5° has a negative polarization in visible [52-55] and radio wave part of the spectrum [58]. However, the diffracted component intensity is relatively low, so the contribution of this mechanism to the resulting negative polarization is small.

4. Coherent Backscattering Enhancement

Interference mechanisms for the formation of negative polarization seem to be the most hopeful, since they are based on the universal multiple scattering mechanism, which takes place in any sufficiently dense medium of scattering particles.

The effect of coherent backscattering (also sometimes referred to in the literature as the "effect of weak localization") of light in discrete random medium was first described by Watson [56]. It is still under active theoretical and laboratory research [57-61]. To find out how the brightness opposition effect is caused by interference, we examine a discrete medium consisting of scattering particles randomly scattered and exposed to a plane wave. We will focus on two backward (conjugate) scattering paths that include the same particle configuration. When the waves scatter, their interference can be constructive or destructive depending on the phase difference between their paths. If the observer is not directly in the backscattering direction, the interference effect is zero due to the random position of the particles. This creates an incoherent intensity. However, when the observer is exactly in the backscattering direction ($\alpha = 0°$), coherence is preserved and the interference is always constructive, resulting in the opposite peak in the intensity of the scattered radiation.

Shkuratov [62,63] was the first to propose a coherent backscattering polarization mechanism. A little later, independently of him, the same mechanism was described by Muinonen [64].

To understand the polarization opposition effect, imagine small particles 1-4 in a plane perpendicular to the direction of the light (see Figure 4). If the incident light is unpolarized, it can be represented as a mixture of two linearly polarized beams. Rayleigh particles (much smaller than the wavelength) scatter light in a plane perpendicular to the incident radiation, with polarized light perpendicular to the scattering plane. Particles 3 and 4 scatter negatively polarized light along conjugated paths, while particles 1 and 2 scatter positively polarized light. Coherent backscattering amplifies the negative polarization contribution at small phase angles, resulting in a negative polarization branch comparable to the brightness opposition effect. The polarization opposition effect is less pronounced than the brightness opposition effect due to the fact that certain particle configurations contribute to it.

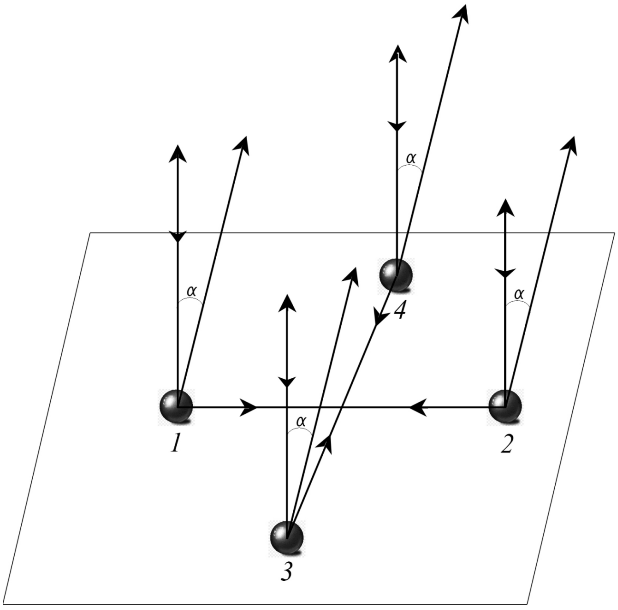

Figure 4. Model of coherent backscattering enhancement. Waves (3-4) and (4-3) always interfere constructively, while waves (1-2) and (2-1) at non-zero phase angles interference can be constructive or destructive depending on the phase difference between their paths.

It should also be mentioned that this mechanism predicts the presence of negative polarization at big phase angles near 180°, since all above considerations, which are valid for the phase angle α, are also valid for the phase angle 180 – α. Despite technical difficulties in measuring the large phase angles polarization, some laboratory polarimetric measurements have shown that negative polarization there is at phase angles α > 170° [65,66]. However, it should be noted that negative polarization at big phase angles is observed in a much narrower range of angles than at small phase angles. This fact suggests that one mechanism of coherent backscattering enhancement cannot explain all the features of scattering, and, most likely, several mechanisms operate simultaneously.

4.1 Model of Double Scattering by a Set of Point Scatterers

Any scattering particle can be described as a number of point scatterers interacting with each other. Therefore, it is logical to try to describe such an interaction theoretically.

The simplest model was developed by Muinonen [64], who considered double scattering between two particles representing electric dipoles. When averaging the second-order scattering matrix over uniformly distributed particles, it was found that a strong negative polarization accompanies the oppositional brightness peak at small phase angles. The value of negative polarization is extremely sensitive to the average distance between particles. However, since dipole particles have a small scattering cross section, the negative polarization and opposition peak disappear when the combined first and second order scattering is considered. However, replacing the dipole scatterer with a dielectric half-space somewhat increases the contribution of second-order scattering [67].

Muinonen investigated the reflection of waves from two curved surfaces [68] and found negative polarization when considering the phase of an electromagnetic field, which cast doubt on Wolf's shading model (Section 3.4).

Shkuratov [69] developed a more general model of light scattering by a set of point scatterers. He considered a medium consisting of little (quasi-Rayleigh) scattering objects restrained by flat interface. The characteristics of the particle were the single-scattering albedo ω, the polarimetrical phase function P(α), and r/λ is the ratio of the average particle size to wavelength. The bulk density of scattering objects is equal to ξ. The model took into account only single and double scattering of light in a medium, which was calculated using the theory of radiative transfer [70-72]. However, despite these assumptions, the expressions for the linear polarization degree turned out to be too complicated [73]. As a result, additional assumptions were made: the phase dependence of single scattering was assumed to be isotropic, and the phase dependence of a quasi-Rayleigh particle was described by the formula $f(\alpha)=G\frac{1-(\cos\alpha)^2}{1+(\cos\alpha)^2}$, where G is the polarimetric scale factor (0 < G < 1). These assumptions made it possible to obtain rather simple relations [73]:

$$P(\alpha)=G\frac{\left(1+2\sqrt{1-\omega}\right)^2}{9}\left(\frac{\sin^2\alpha}{1+\cos^2\alpha}+\frac{2\omega\xi\left[1-\sqrt{1+\left(\frac{8}{5}\rho\sin\frac{\alpha}{2}\right)^2}\right]}{\left(\frac{8}{5}\rho\sin\frac{\alpha}{2}\right)^2\sqrt{1+\left(\frac{8}{5}\rho\sin\frac{\alpha}{2}\right)^2}\ln(1-\xi)}\right) \quad (5)$$

where $\rho=\frac{8\pi r\ln(1-\xi)}{3\lambda}$, r is the average particle size, λ is wavelength, ξ is bulk density of scattering objects, ω is single-scattering albedo. When deriving Equation (5), it was also assumed that shading has the same effect on double and single scattering. The second and first order polarization originates due to scattering objects that form the surface relief. For certain sets of parameters, Equation (5) describes quite well the symmetric branch of negative polarization, which is characteristic of many celestial objects, such as the Moon [2], comets [74], or asteroids [75].

4.2 Vector Theory of Coherent Backscatter Enhancement

The first attempt to carry out a theoretical calculation of the opposition effect of polarization, based on the coherent backscattering vector theory, was carried out by Mishchenko [76]. It was based on formulas obtained by Ozrin [77] for a semi-infinite medium consisting of Rayleigh scattering objects with zero absorption. Despite the thoroughness of the theory, the final result gave only asymptotic expressions applicable to extremely small and large phase angles. Thus, the full effect of the angular polarization opposition, including the exact position and magnitude of the polarization minimum, remained unknown. However, later an exact solution was obtained [78], subsequently adapted to the Stokes vectors formalism [79].

Authors considered a semi-infinite homogeneous random medium consisting of Rayleigh scattering objects with zero absorption, using the standard set of Stokes parameters to determine the polarization state of the scattered and incident light in meridional planes (the planes containing the scattering object, the light source, and the perpendicular to the boundary environment) [80]. It was assumed that the matrix of scattering is as follows:

-ORDER POINT-S $$\mathbf{F}(\alpha)=\begin{bmatrix} F_{11}(\alpha) & F_{12}(\alpha) & 0 & 0 \\ F_{21}(\alpha) & F_{22}(\alpha) & 0 & 0 \\ 0 & 0 & F_{33}(\alpha) & 0 \\ 0 & 0 & 0 & F_{44}(\alpha) \end{bmatrix}, \quad (6)$$

where $F_{ij}(\alpha)$ are elements of scattering matrix, depending on phase angle α.

F(α) can be represented as the sum of following terms:

$$\mathbf{F}(\alpha)=\mathbf{F}^{1}(\alpha)+\mathbf{F}^{L}(\alpha)+\mathbf{F}^{C}(\alpha), \quad (7)$$

where $\mathbf{F}^1(\alpha)$ takes into account the contribution of single scattering, $\mathbf{F}^L(\alpha)$ represents 2nd order or higher ladder scatterplots and $\mathbf{F}^C(\alpha)$ represents 2nd order or higher cyclic scatterplots. To simplify the analysis at small phase angles, the angular parameter q = k*l*α is introduced, where *l* is the mean free path of photons in the scattering medium and k is the wavenumber. As a result, the following relations are obtained for these matrices:

$$\mathbf{F}^{1}(\alpha)\approx\mathbf{F}^{1}(0)=\frac{3}{16}\begin{bmatrix} 1 & 0 & 0 & 0 \\ 0 & 1 & 0 & 0 \\ 0 & 0 & -1 & 0 \\ 0 & 0 & 0 & -1 \end{bmatrix}, \quad (8)$$

$$\mathbf{F}^{L}(\alpha)\approx\mathbf{F}^{L}(0)=\frac{1}{4}\begin{bmatrix} \gamma_{11}(0)+\gamma_{12}(0) & 0 & 0 & 0 \\ 0 & \gamma_{11}(0)-\gamma_{12}(0) & 0 & 0 \\ 0 & 0 & \gamma_{12}(0)-\gamma_{11}(0) & 0 \\ 0 & 0 & 0 & \gamma_{44}(0) \end{bmatrix}-\mathbf{F}^{1}(0), \quad (9)$$

$$\mathbf{F}^{C}(\alpha)\approx\mathbf{F}^{C}(q)=\begin{bmatrix} F_{11}^{C}(q) & F_{12}^{C}(q) & 0 & 0 \\ F_{12}^{C}(q) & F_{22}^{C}(q) & 0 & 0 \\ 0 & 0 & F_{33}^{C}(q) & 0 \\ 0 & 0 & 0 & F_{44}^{C}(q) \end{bmatrix}-\mathbf{F}^{1}(0), \quad (10)$$

where

$$F_{11}^{C}(q)=\frac{1}{8}\left[\gamma_{11}(q)+\gamma_{22}(q)-\gamma_{33}(q)+\gamma_{44}(q)\right], \quad (11)$$

$$F_{22}^{C}(q)=\frac{1}{8}\left[\gamma_{11}(q)+\gamma_{22}(q)+\gamma_{33}(q)-\gamma_{44}(q)\right], \quad (12)$$

$$F_{33}^{C}(q)=\frac{1}{8}\left[\gamma_{33}(q)+\gamma_{44}(q)\right]-\frac{1}{4}\gamma_{12}(q), \quad (13)$$

$$F_{44}^{C}(q)=\frac{1}{8}\left[\gamma_{33}(q)+\gamma_{44}(q)\right]+\frac{1}{4}\gamma_{12}(q), \quad (14)$$

$$F_{12}^{C}(q)=\frac{1}{8}\left[\gamma_{11}(q)-\gamma_{22}(q)\right], \quad (15)$$

where γ_{ij}(q)—angular functions.

Explicit expressions for γ_{ij}(q) are unknown, but they can be calculated numerically, in accordance with the special procedure [78]. Using the above relations, one can obtain the all Stokes matrix at any values of q. If, in addition, we know *l*, the Stokes matrix can be represented as a function of α rather than q. And knowing the Stokes matrix, it is easy to calculate the linear polarization degree:

$$P(\alpha)=-\frac{Q(\alpha)}{I(\alpha)}=-\frac{F_{12}^{C}(q)}{F_{11}^{1}(0)+F_{11}^{L}(0)+F_{11}^{C}(q)}. \quad (16)$$

It was shown by Mishchenko et al. [79] that, in accordance with this theory, the coherent enhancement of backscattering induces a rather narrow and highly asymmetric negative polarization branch, similar to the negative polarization branches observed for a number of celestial bodies, such as the rings of Saturn [76] and Galilean satellites Jupiter [19].

5. Effects of Near Field

When a particle or system of particles close in size to the wavelength is nearby, the wave becomes highly non-uniform due to the delay of the electromagnetic wave inside the particle compared to the incident wave. In such a wave, the surfaces of constant phase and amplitude do not coincide, and the amplitude, polarization, and direction of propagation depend on the position relative to the scatterer. According to the Lorentz-Mie theory, calculations for spherical particles show that the surface of the constant phase of the wave takes the form of a funnel near the particle if its size is close to the wavelength [81]. Thus, neighboring particles are affected by the variegated field and therefore scattered light exhibits special features. It was shown by Petrova et al. [82] that the rotation of the field vector in the proximity of the particle reduces the scattering intensity in the backscattering and forward scattering regions and causes negative polarization. These features of light scattering are called “near field effects” [83].

The near field effect is effective in densely packed environments at various angles. However, for large scatterers in homogeneous and isotropic media, it becomes negligible, since the inhomogeneity scale is similar to the wavelength. Similarly, if the scatterers are smaller than the wavelength, the near field effect can also be neglected due to the small wave inhomogeneity.

The effectiveness of the near field effect is highest in media with scatterers close to the wavelength, or in polydisperse media, where larger particles cause wave inhomogeneities for smaller particles. Further investigation shows that the effect of the near field effect is highly dependent on particle size, refractive index, interparticle spacing, and phase angle [84].

However, the realism of this mechanism is called into question by some researchers [85]. In particular, they pointed out that the name of this effect was chosen poorly, because in the classical literature [86] the “near field” is a field whose amplitude decreases faster than $1/r$, where r is the distance to the wave source. In the description of this mechanism, the near field is understood as any field in the immediate proximity of the scattering particle. In addition, the field near the particle is the result of the interference of the scattered and incident radiation, as a result of which this field has both a longitudinal and a transverse component. And in the course of describing the effect of near field, only the transverse component of the electromagnetic field is considered, while the longitudinal component is ignored. Thus, the description of this mechanism is at least incomplete.

Also measurements of the linear polarization degree in the laboratory of a medium consisting of hematite particles 1-2 μm in size were carried out [85]. Previous laboratory measurements of individual particles of hematite [36] showed the existence of a negative branch of polarization. While in a medium consisting of such particles, negative polarization was not found at all, which contradicts the assertions that near-field effects enhance negative polarization.

Also a light scattering computer simulation for particles cluster was carried out using the method of discrete-dipole approximations [85]. It was shown by Petrova et al. [82] that taking into account double scattering leads to the appearance of negative polarization even in the case when the singly scattered light is positively polarized. Computer simulation was carried out for particles of the same parameters (sizes and refractive indices), but taking into account all scattering orders. And as a result, negative polarization could not be detected.

However, it was shown by Petrova et al. [87] that the experimental data and model calculations described by Shkuratov and Zubko [85] do not disprove the significance of the influence of the near field on scattering mechanisms. The backscattering coherent enhancement works on sparse media, while the near field effect appears in very densely packed media. For this reason, it cannot be concluded that the near field effects are insignificant in the surface layer of a dark scattering medium. Although the effect of coherent backscattering is well known, the theory of the near field effect is not yet complete and its contribution to backscattering is still difficult to quantify. Despite these problems, Petrova et al. [87] stated that the near field effect is indeed a workable mechanism and cannot be triggered due to the discovery of dense media in studies.

6. Conclusions

The paper presents a literature review of the main mechanisms, the cumulative action of which explains the occurrence of the negative branch of the linear polarization degree of scattered light. The paper discusses the results of ground-based observations of the negative branch of the degree of linear polarization for various objects of the solar system. Scattering by single particles, shadow effect, coherent backscattering enhancement, and effects of near field are considered. The advantages and disadvantages of each of the described mechanisms are considered in detail. The review will be useful to all researchers studying the scattering of light by celestial bodies.

Funding

Work is supported by the Ministry of Science and Higher Education of the RF (grant 075-15-2020-780).

Acknowledgment

Author acknowledges the support from the Ministry of Science and Higher Education of the RF (grant 075-15-2020-780).

Data Availability Statement

The data that support the findings of this study are available from the author, upon reasonable request.

Conflict of Interest

There is no conflict of interest.

References

[1] Shkuratov, Y., Ovcharenko, A., Zubko, E., et al., 2002. The opposition effect and negative polarization of structural analogs for planetary regoliths. Icarus. 159(2), 396-416.

[2] Lyot, B., 1929. Recherches sur la polarisation de la lumiere des planetes et de queldues substances terrestres (French) [Research on the polarization of the light of planets and certain terrestrial substances]Ann Obs Meudon. 8, 1-161.

[3] Bowell, E., Dollfus, A., Geake, J.E., 1972. Polarimetric properties of the lunar surface and its interpretation. Part 5: Apollo 14 and Luna 16 lunar samples. Proceedings of the Lunar Science Conference. 3, 3103.

[4] Ovcharenko, A.A., Shkuratov, Y.G., 2000. Weak-localization effect for light backscattered by surfaces with a complex structure. Optics and Spectroscopy. 88, 253-259.

[5] Ohman Y., 1955. A tentative explanation of the polarization in diffuse reflection. Stockholm Observatory Annual. 18, 1-10.

[6] McCoyd, G.C., 1967. Polarization properties of a simple dielectric rough-surface model. Journal of the Optical Society of America. 57(11), 1345-1350.

[7] Hopfield, J.J., 1966. Mechanism of lunar polarization. Science. 151(3716), 1380-1381.

[8] Veverka J., 1977. Polarimetry of satellite surfaces. Planetary satellites. University of Arizona Press: Tucson. pp. 210-231.

[9] Petrova, E.V., Tishkovets, V.P., 2011. Light scattering by morphologically complex objects and opposition effects (a review). Solar System Research. 45(4), 304.

[10] Noebauer, U.M., Sim, S.A., 2019. Monte Carlo radiative transfer. Living Reviews in Computational Astrophysics. 5, 1-103.

[11] Mishchenko, M.I., Rosenbush, V.K., Kiselev, N.N., et al., 2010. Polarimetric remote sensing of solar system objects. arXiv preprint arXiv:1010.1171.

[12] Lyot, B., 1964. Research on the polarization of light from planets and from some terrestrial substances. National Aeronautics and Space Administration: Washington.

[13] Coyne, G.V., Pellicori, S.F., 1970. Wavelength dependence of polarization. xx. the integrated disk of the moon. Astronomical Journal. 75, 54.

[14] Dollfus, A., Bowell, E., 1971. Polarimetric properties of the lunar surface and its interpretation. Part I. Telescopic observations. Astronomy and Astrophysics. 10, 29.

[15] Veverka, J., 1971. Polarization measurements of the Galilean satellites of Jupiter. Icarus. 14(3), 355-359.

[16] Dollfus, A., 1975. Optical polarimetry of the Galilean satellites of Jupiter. Icarus. 25(3), 416-431.

[17] Rosenbush, V.K., Avramchuk, V.V., Rosenbush, A.E., et al., 1997. Polarization properties of the Galilean satellites of Jupiter: Observations and preliminary analysis. The Astrophysical Journal. 487(1), 402.

[18] Rosenbush, V.K., Kiselev, N.N., Jockers, K., et al., 2000. Optical polarimetry of the Galilean satellites, Iapetus, and 64 Angelina near opposition. Kinematika i Fizika Nebesnykh Tel Supplement. 3, 227-230.

[19] Kiselev, N., Rosenbush, V., Muinonen, K., et al., 2022. New polarimetric data for the galilean satellites: Europa observations and modeling. The Planetary Science Journal. 3(6), 134.

[20] Rosenbush, V.K., 2002. The phase-angle and longitude dependence of polarization for Callisto. Icarus. 159(1), 145-155.

[21] Rosenbush, V.K., Kiselev, N.N., 2005. Polarization opposition effect for the Galilean satellites of Jupiter. Icarus. 179(2), 490-496.

[22] Zellner, B., 1972. Minor planets and related objects. VIII. Deimos. The Astronomical Journal. 77, 183.

[23] Bowell, E., Zellner, B., 1974. Polarizations of asteroids and satellites. University Arizona Press: Tucson. pp. 381-404.

[24] Kiselev, N.N., Chernova, G.P., 1981. Phase functions of polarization and brightness and the nature of cometary atmosphere particles. Icarus. 48(3), 473-481.

[25] Mukai, S., Mukai, T., Kikuchi, S. (editors), 1991. Scattering properties of cometary dust based on polarimetric data. Origin and Evolution of Interplanetary Dust: Proceedings of the 126th Colloquium of the International Astronomical Union; 1990 Aug 27-30; Kyoto. Netherlands: Springer. p. 249-252.

[26] Chernova, G.P., Kiselev, N.N., Jockers, K., 1993. Polarimetric characteristics of dust particles as observed in 13 comets: Comparisons with asteroids. Icarus. 103(1), 144-158.

[27] Levasseur-Regourd, A.C., Hadamcik, E., Renard, J.B., 1996. Evidence for two classes of comets from their polarimetric properties at large phase angles. Astronomy and Astrophysics. 313, 327-333.

[28] Dlugach, J.M., Ivanova, O.V., Mishchenko, M.I., et al., 2018. Retrieval of microphysical characteristics of particles in atmospheres of distant comets from ground-based polarimetry. Journal of Quantitative

Spectroscopy and Radiative Transfer. 205, 80-90.
[29] Halder, P., Ganesh, S., 2021. Modelling heterogeneous dust particles: An application to cometary polarization. Monthly Notices of the Royal Astronomical Society. 501(2), 1766-1781.
[30] Lyot, B., 1934. Polarisation des petites planets (French) [Polarization of minor planets]. Comptes Rendus de l'Académie des Sciences. 199, 774.
[31] Zellner, B., Gehrels, T., Gradie, J., 1974. Minor planets and related objects. XVI-Polarimetric diameters. The Astronomical Journal. 79, 1100-1110.
[32] Zellner, B., Gradie, J., 1976. Polarization of the reflected light of asteroid 433 Eros. Icarus. 28(1), 117-123.
[33] Grynko, Y., Shkuratov, Y., Alhaddad, S., et al., 2022. Negative polarization of light at backscattering from a numerical analog of planetary regoliths. Icarus. 384, 115099.
[34] Bohren, C.F., Huffman, D.R., 1998. Absorption and scattering of light by small particles. Wiley-VCH: Weinheim.
[35] Kiselev, N.N., Chernova, G.P., 1976. On a possible new version of the polarization-phase relation for comets. Astronomicheskij Tsirkulyar. 931, 5-7.
[36] Muñoz, O., Volten, H., Hovenier, J.W., et al., 2006. Experimental and computational study of light scattering by irregular particles with extreme refractive indices: Hematite and rutile. Astronomy & Astrophysics. 446(2), 525-535.
[37] Muñoz, O., Hovenier, J.W., 2011. Laboratory measurements of single light scattering by ensembles of randomly oriented small irregular particles in air. A review. Journal of Quantitative Spectroscopy and Radiative Transfer. 112(11), 1646-1657.
[38] Zubko, E., Petrov, D., Shkuratov, Y., et al., 2005. Discrete dipole approximation simulations of scattering by particles with hierarchical structure. Applied Optics. 44(30), 6479-6485.
[39] Steigmann, G.A., 1978. A polarimetric model for a dust-covered planetary surface. Monthly Notices of the Royal Astronomical Society. 185(4), 877-888.
[40] Steigmann, G.A., 1984. Application of a polarimetric model to the surface microstructure of particles in the B-ring of Saturn. Monthly Notices of the Royal Astronomical Society. 209(2), 359-371.
[41] Steigmann, G.A., 1986. Optical polarimetry of sulphur and the surface microstructure of Io. Monthly Notices of the Royal Astronomical Society. 219(4), 823-833.
[42] Steigmann, G.A., Dodsworth, M.B., 1987. Surface microstructure of the nucleus of Comet P/Halley. The Observatory. 107, 263-267.
[43] Shkuratov, Y.G., Muinonen, K., Bowell, E., et al., 1994. A critical review of theoretical models of negatively polarized light scattered by atmosphereless solar system bodies. Earth Moon and Planets. 65(3), 201-246.
[44] Wolff, M., 1975. Polarization of light reflected from rough planetary surface. Applied Optics. 14(6), 1395-1405.
[45] Wolff, M., 1980. Theory and application of the polarization-albedo rules. Icarus. 44(3), 780-792.
[46] Wolff, M., 1981. Computing diffuse reflection from particulate planetary surface with a new function. Applied Optics. 20(14), 2493-2498.
[47] Geake, J.E., Geake, M., Zellner, B.H., 1984. Experiments to test theoretical models of the polarization of light by rough surfaces. Monthly Notices of the Royal Astronomical Society. 210(1), 89-112.
[48] Dollfus, A., Wolff, M. (editors), 1981. Theory and application of the negative branch of polarization for airless planetary objects. Lunar and Planetary Science Conference; 1981 Mar 16-20; Houston. p. 232-234.
[49] Dollfus, A., Wolff, M., Geake, J.E., et al., 1989. Photopolarimetry of asteroids. Asteroids Ii. 594-616.
[50] Shkuratov, Y.G., 1982. A model for negative polarization of light by cosmic bodies without atmospheres. Soviet Astronomy. 26, 493-496.
[51] Shkuratov, I.G., Kreslavskii, M.A., Opanasenko, N.V., 1992. Analysis of a mechanism of the negative polarization of light scattered by atmosphereless celestial bodies. Astronomicheskii Vestnik. 26, 46-53.
[52] Jentzsch, F., 1927. Über die Beugung des Lichtes an Stahlschneiden (German) [On the diffraction of light on steel cutting edges]. Annalen der Physik. 389(18), 292-312.
[53] Wolfsohn G., 1928. Strenge theorie der interferenz und beugung (German) [Strict theory of interference and diffraction]. Handbuch der Physik. Springer Verlag: Berlin. pp. 263-316.
[54] Savornin, J., 1939. Étude de la diffraction éloignée (French) [Study of distant diffraction]. Annales de Physique. 11(11), 129-255.
[55] Horton, C.W., Watson, R.B., 1950. On the diffraction of radar waves by a semi-infinite conducting screen. Journal of Applied Physics. 21(1), 16-21.
[56] Watson, K.M., 1969. Multiple scattering of electromagnetic waves in an underdense plasma. Journal of Mathematical Physics. 10(4), 688-702.

[57] Akkermans, E., Wolf, P.E., Maynard, R., et al., 1988. Theoretical study of the coherent backscattering of light by disordered media. Journal de Physique. 49(1), 77-98.

[58] Barabanenkov, Y.N., Kravtsov, Y.A., Ozrin, V.D., et al., 1991. II enhanced backscattering in optics. Progress in optics. 29, 65-197.

[59] Mishchenko, M.I., Dlugach, J.M., Liu, L., 2009. Azimuthal asymmetry of the coherent backscattering cone: Theoretical results. Physical Review A. 80(5), 053824.

[60] Zhou, C., 2018. Coherent backscatter enhancement in single scattering. Optics Express. 26(10), A508-A519.

[61] Gorodnichev, E.E., Kondratiev, K.A., Rogozkin, D.B., 2022. Coherent backscattering of light from a Faraday medium. Physical Review B. 105(10), 104208.

[62] Shkuratov, Y.G., 1985. On opposition brightness surge and light negative polarization of solid cosmic surfaces. Astronomicheskij Tsirkulyar. 1400, 1.

[63] Shkuratov, I.G., 1988. The nature of the polarimetric inhomogeneity of the surface of the asteroid 4 Vesta. Astronomicheskii Vestnik. 22, 152-158.

[64] Muinonen, K. (editor), 1989. Electromagnetic scattering by two interacting dipoles. The 1989 URSI International Symposium on Electromagnetic Theory; 1989 Aug 14-17; Stockholm. p. 428-430.

[65] Frattin, E., Muñoz, O., Moreno, F., et al., 2019. Experimental phase function and degree of linear polarization of cometary dust analogues. Monthly Notices of the Royal Astronomical Society. 484(2), 2198-2211.

[66] Muñoz, O., Moreno, F., Gómez-Martín, J.C., et al., 2020. Experimental phase function and degree of linear polarization curves of millimeter-sized cosmic dust analogs. The Astrophysical Journal Supplement Series. 247(1), 19.

[67] Muinonen, K.O., Sihvola, A.H., Lindell, I.V., et al., 1991. Scattering by a small object close to an interface. II. Study of backscattering. Journal of the Optical Society of America A. 8(3), 477-482.

[68] Muinonen K., 1990. Light scattering by inhomogeneous media: Backward enhancement and reversal of linear polarization [PhD thesis]. Helsinki: University of Helsinki.

[69] Shkuratov, I.G., 1991. An interference model of the negative polarization of light scattered by solid surfaces of celestial bodies. Astronomicheskii Vestnik. 25, 152-161.

[70] Hapke, B.W., 1963. A theoretical photometric function for the lunar surface. Journal of Geophysical Research. 68(15), 4571-4586.

[71] Hapke, B., 1993. Theory of reflectance and emittance spectroscopy. Cambridge University Press: Cambridge.

[72] Hapke, B., 2008. Bidirectional reflectance spectroscopy: 6. Effects of porosity. Icarus. 195(2), 918-926.

[73] Shkuratov, Y.G., Melkumova, L.Y., 1991. Diffraction model of the negative polarization of light scattering by atmosphereless cosmic bodies. Lunar and Planetary Science Conference. 22, 1243.

[74] Zhuzhulina, E., Petrov, D., Kiselev, N., et al., 2022. Aperture polarimetry of selected comets in 2018-2020: Observations and computer simulation. Journal of Quantitative Spectroscopy and Radiative Transfer. 290, 108321.

[75] Petrov, D., Kiselev, N., 2018. Computer simulation of position and maximum of linear polarization of asteroids. Journal of Quantitative Spectroscopy and Radiative Transfer. 204, 88-93.

[76] Mishchenko, M.I., 1993. On the nature of the polarization opposition effect exhibited by Saturn's rings. The Astrophysical Journal. 411, 351-361.

[77] Ozrin, V.D., 1992. Exact solution for coherent backscattering of polarized light from a random medium of Rayleigh scatterers. Waves in Random Media. 2(2), 141.

[78] Amic, E., Luck, J.M., Nieuwenhuizen, T.M., 1997. Multiple Rayleigh scattering of electromagnetic waves. Journal de Physique I. 7(3), 445-483.

[79] Mishchenko, M.I., Luck, J.M., Nieuwenhuizen, T.M., 2000. Full angular profile of the coherent polarization opposition effect. Journal of the Optical Society of America A. 17(5), 888-891.

[80] Mishchenko, M.I., 1996. Diffuse and coherent backscattering by discrete random media-I. Radar reflectivity, polarization ratios, and enhancement factors for a half-space of polydisperse, nonabsorbing and absorbing spherical particles. Journal of Quantitative Spectroscopy and Radiative Transfer. 56(5), 673-702.

[81] Tishkovets, V.P., 1998. Backscattering of light by close-packed systems of particles. Optics and Spectroscopy. 85(2), 212-217.

[82] Petrova, E.V., Tishkovets, V.P., Jockers, K., 2007. Modeling of opposition effects with ensembles of clusters: Interplay of various scattering mechanisms. Icarus. 188(1), 233-245.

[83] Tishkovets, V.P., 2008. Light scattering by closely packed clusters: Shielding of particles by each other

in the near field. Journal of Quantitative Spectroscopy and Radiative Transfer. 109(16), 2665-2672.
[84] Tishkovets, V., Litvinov, P., Petrova, E., et al., 2005. Backscattering effects for discrete random media: theoretical results. Photopolarimetry in remote sensing. Springer: Netherlands. pp. 221-242.
[85] Shkuratov, Y.G., Zubko, E.S., 2008. Comment on "Modeling of opposition effects with ensembles of clusters: Interplay of various scattering mechanisms" by Elena V. Petrova, Victor P. Tishkovets, Klaus Jockers, 2007 [Icarus 188, 233-245]. Icarus. 194(2), 850-852.
[86] Born, M., Wolf, E., 1999. Principles of optics. Cambridge University Press: Cambridge.
[87] Petrova, E.V., Tishkovets, V.P., Jockers, K., 2008. Rebuttal to comment on "Modeling of opposition effects with ensembles of clusters: Interplay of various scattering mechanisms" by Elena V. Petrova, Victor P. Tishkovets, Klaus Jockers, 2007 [Icarus 188, 233-245]. Icarus. 194(2), 853-856.